A HIGH-ORDER MIXTURE MODEL FOR PERIODIC PARTICULATE COMPOSITES

A. TOLEDANO and H. MURAKAMI

Department of Applied Mechanics and Engineering Sciences, University of California,
San Diego, La Jolla, CA 92093, U.S.A.

Abstract—A deterministic mixture theory is presented for periodic particulate composites. The model is constructed by introducing convenient microdisplacement and microstress variables, and by using a regular asymptotic technique with multiple scales. Governing equations and appropriate boundary conditions are then deduced from Reissner's mixed variational principle (*J. Math. Phys.* **29**, 90–95 (1950)). In order to test the accuracy of the present model, harmonic wave propagation is examined and compared with available experimental data for glass/epoxy and steel/PMMA composites reported by Kinra and Ker (*Int. J. Solids Structures* **19**, 393–410 (1983)). Also, the effective elastic moduli are computed, and the results compared with other analytical methods.

1. INTRODUCTION

Composite materials exhibit very different behavior under static and dynamic loads, as compared to homogeneous isotropic solids. Therefore, proper assessment of the composite's physical properties, such as elastic moduli and wave spectra, is important for most engineering applications.

Different analytical methods for the determination of the effective elastic moduli of particulate composites have been compiled by Christensen[1]. These are: (i) the variational approach based on extremum principles[2–5], (ii) the probabilistic approach[6–9], and (iii) the self-consistent scheme[10–13]. The estimates of effective moduli which elucidate the effect of the geometry of inclusion were presented by Nemat-Nasser and co-workers[14, 15]. At this moment it is safe to conclude that formulas are available which predict accurately the effective elastic moduli of the composites.

In order to clarify dynamic behaviors of particulate composites ultrasonic measurements of longitudinal and shear wave velocities have been recorded by Kinra *et al.*[16] at low frequency, and by Kinra and Anand[17] at long and short wavelengths for random particulate composites. Later, Kinra and Ker[18], again using ultrasonic devices, measured longitudinal wave speeds at low and high frequencies for periodic particulate composites. Their experimental investigation revealed the existence of stop and pass bands in the periodic composites[18], which were totally absent in the random composites[16, 17]. The existence of stop and pass bands was predicted analytically in the transmission of harmonic waves through periodic three-dimensional composites by Minagawa and Nemat-Nasser[19] who used a quotient method to compute phase velocity spectra. It is noted that phase velocity data provide an accuracy measure of dispersive continuum models and therefore such data are of considerable importance.

The dynamic behavior of random particulate composites has been studied theoretically via harmonic wave propagation. Mal and Bose[20], using a probabilistic approach, gave values for the effective wave speeds for imperfectly bonded spheres randomly dispersed in the matrix. Their analysis is confined to the long wavelength range. Datta[21] obtained longitudinal wave velocities through the scattering of a plane P-wave by a distribution of rigid spheroids. Later, Datta[22], using a probabilistic approach similar to that in Ref. [21], computed longitudinal and shear wave speeds for the case of identical elastic ellipsoids. His results[22] are however nondispersive, since the calculations stem from a long wavelength approximation but reproduces an appropriate bound of Ref. [3]. Dispersive models for random particulate composites have been proposed by Beltzer *et al.*[23] for a viscoelastic

matrix, with dilute particle concentration, and by Ben-Amoz[24] using asymptotic expansions to derive governing equations for the macro-motion. The latter model fails to predict the experimental data reported later by Kinra and Ker[18]. Gaunard and Überall[25] have also presented a dispersive model for random particle distribution at low concentrations using scattering theory.

A deterministic continuum model is presented here for the simulation of harmonic wave propagation through periodic particulate composites. This method has been successfully applied to angle-ply laminates[26] and fiber-reinforced composites[27]. It consists in using a regular asymptotic technique with multiple scales to derive appropriate trial displacement and stress fields. This procedure yields a sequence of microboundary value problems (MBVPs) defined over a unit cell, which characterizes the periodicity of the composite microstructure. Governing equations and boundary conditions are then deduced from Reissner's mixed variational principle[28]. The lowest order model of this MBVP method is equivalent to the "$O(1)$ homogenization theory", by Bensoussan et al.[29] and Sanchez-Palencia[30]. This gives the effective elastic moduli. However, for dynamic problems where the wavelength is of the same order of magnitude as the inclusion's dimensions, a higher order model is necessary to simulate wave dispersion spectra. Such a theory is named an $O(\varepsilon)$ (at least) homogenization theory, where ε denotes a typical ratio of micro-to-macrodimensions of the composite. This method of two-space homogenization has also been applied by Burridge and Keller[31] to derive the equations describing the macroscopic behavior of fluid-filled porous media. However, numerical results were not presented in their work.

Following the derivation of the mixture model, propagation of harmonic waves through periodic particulate composites is examined using the approach outlined above, and the results are compared with the experimental data recorded by Kinra and Ker[18] for glass/epoxy and steel/PMMA composites. Also, in the limit when $\varepsilon \to 0$, the effective elastic moduli are computed and compared with Hashin's results[2]. In all cases, good agreement is observed between the available experimental data and analytical methods.

2. FORMULATION

Consider a volume $\bar{V}$ which contains spherical particles periodically distributed within the matrix, as shown in Fig. 1. This volume is referred to a Cartesian coordinate system $\bar{x}_1$, $\bar{x}_2$, $\bar{x}_3$.

The following notation: $(\ )^{(\alpha)}, \alpha = 1, 2$ will designate quantities associated with material α, such that $\alpha = 1$ represents the particle and $\alpha = 2$ the matrix. Barred and unbarred quantities will be associated with dimensional and non-dimensional variables, respectively. Unless otherwise specified, the usual Cartesian indicial notation is employed where latin indices range from 1 to 3 and repeated indices imply the summation convention. Also, $(\ )_{,i}$ and $(\ )_{,t}$ are used to denote partial differentiation with respect to $\bar{x}_i$ and time $\bar{t}$, respectively.

With the help of the foregoing notation, the governing equations for the displacement vector $\bar{u}_i^{(\alpha)}$ and stress tensor $\bar{\sigma}_{ij}^{(\alpha)}$ associated with the αth-constituent are:
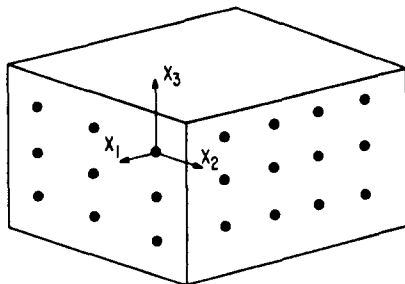

Fig. 1. A periodic particulate composite.

(a) equations of motion

$$\bar{\sigma}^{(\alpha)}_{ji,j} = \bar{\rho}^{(\alpha)}\bar{u}^{(\alpha)}_{i,tt}, \qquad \bar{\sigma}^{(\alpha)}_{ji} = \bar{\sigma}^{(\alpha)}_{ij} \tag{1}$$

where $\bar{\rho}^{(\alpha)}$ represents the mass density;

(b) constitutive equations for isotropic constituents

$$\bar{\sigma}^{(\alpha)}_{ij} = \bar{\lambda}^{(\alpha)}e^{(\alpha)}_{kk}\,\delta_{ij} + 2\bar{\mu}^{(\alpha)}e^{(\alpha)}_{ij} \tag{2}$$

where $\bar{\lambda}^{(\alpha)}$, $\bar{\mu}^{(\alpha)}$ are Lame's constants, $e^{(\alpha)}_{ij}$ the infinitesimal strain tensor and δ_{ij} the Kronecker delta;

(c) strain–displacement relations

$$e^{(\alpha)}_{ij} = \tfrac{1}{2}(\bar{u}^{(\alpha)}_{i,j} + \bar{u}^{(\alpha)}_{j,i}); \tag{3}$$

(d) interface continuity conditions

$$\bar{u}^{(1)}_i = \bar{u}^{(2)}_i, \qquad \bar{\sigma}^{(1)}_{ji}v^{(1)}_j = \bar{\sigma}^{(2)}_{ji}v^{(1)}_j \quad \text{on} \quad \bar{A}_1 \tag{4}$$

where $\bar{A}_1$ denotes the particle–matrix interface surface;

(e) initial conditions at $\bar{t} = 0$ and appropriate boundary conditions along the boundary $\partial\bar{V}$.

Conditions (a)–(e) constitute an initial boundary value problem. However, due to the large number of heterogeneities in the medium, its direct solution represents a formidable task. The purpose of the following analysis is to circumvent this difficulty by deriving a set of partial differential equations with constant coefficients, the solution of which will thus represent an approximation to the original problem. To this end, the basic equations are nondimensionalized by introducing the following parameters:

$\bar{\Lambda}$	typical macrosignal wavelength
$\bar{\Delta}$	typical particle spacing or cell dimension
$\bar{C}_{(m)}, \bar{\rho}_{(m)}$	reference wave velocity and macromass density
$\bar{E}_{(m)} \equiv \bar{\rho}_{(m)}\bar{C}^2_{(m)}$	reference modulus
$\bar{t}_{(m)} \equiv \bar{\Lambda}/\bar{C}_{(m)}$	typical macrosignal travel time
$\varepsilon \equiv \bar{\Delta}/\bar{\Lambda}$	ratio of micro-to-macrodimension.

With the help of these parameters, non-dimensional variables are now defined, such that

$$x_i = \frac{\bar{x}_i}{\bar{\Lambda}}, \qquad t = \frac{\bar{t}}{\bar{t}_{(m)}}, \qquad u^{(\alpha)}_i = \frac{\bar{u}^{(\alpha)}_i}{\bar{\Lambda}}$$

$$(\lambda,\mu,\sigma_{ij})^{(\alpha)} = \frac{1}{\bar{E}_{(m)}}\,(\bar{\lambda},\bar{\mu},\bar{\sigma}_{ij})^{(\alpha)}, \qquad \rho^{(\alpha)} = \frac{\bar{\rho}^{(\alpha)}}{\bar{\rho}_{(m)}}. \tag{5}$$

The material properties are periodic in the x_i-space in which the periodicity can be characterized by the cell. This representation implies that stress and displacement fields will vary according to two basic length scales: (1) a macro length characteristic of the body size, and (2) a micro length characteristic of the cell spatial dimensions. Further, in most applications of interest, the microscale is much smaller than the macroscale. Therefore, it appears convenient to use an asymptotic technique based on the two scales involved in the problem. To this end, new independent microcoordinates are introduced, such that

$$x_i^* = \frac{x_i}{\varepsilon}.$$

(6)

As a consequence, all field variables now become functions of both the macrovariables x_i and microvariables x_i^*

$$F(x_i, t) = F^*(x_i, x_j^*, t; \varepsilon).$$

(7a)

Spatial derivatives of such a function F then take the form

$$F_{,i}(x_j, t) = F_{,i}^*(x_j, x_k^*, t; \varepsilon) + \frac{1}{\varepsilon} F_{,i^*}^*(x_j, x_k^*, t; \varepsilon)$$

(7b)

where $(\ )_{,i^*}$ is used to denote partial differentiation with respect to x_i^*. For notational simplicity, F^* will be written as F in what follows.

Applying eqns (5) and (7b) to eqns (1)–(4) yields a new set of "synthesized" governing equations, given by:

(a) equations of motion

$$\sigma_{ji,j}^{(\alpha)} + \frac{1}{\varepsilon}\sigma_{ji,j^*}^{(\alpha)} = \rho^{(\alpha)}u_{i,tt}^{(\alpha)}, \qquad \sigma_{ji}^{(\alpha)} = \sigma_{ij}^{(\alpha)};$$

(8a, b)

(b) constitutive equations for isotropic constituents

$$\sigma_{ij}^{(\alpha)} = \lambda^{(\alpha)}e_{kk}^{(\alpha)}\delta_{ij} + 2\mu^{(\alpha)}e_{ij}^{(\alpha)};$$

(9)

(c) strain–displacement relations

$$e_{ij}^{(\alpha)} = \frac{1}{2}\left[u_{i,j}^{(\alpha)} + u_{j,i}^{(\alpha)} + \frac{1}{\varepsilon}(u_{i,j^*}^{(\alpha)} + u_{j,i^*}^{(\alpha)})\right];$$

(10)

(d) interface continuity conditions

$$u_i^{(1)} = u_i^{(2)}, \qquad \sigma_{ji}^{(1)}v_j^{(1)} = \sigma_{ji}^{(2)}v_j^{(1)} \quad \text{on} \quad A_1.$$

(11a, b)

The periodicity condition implies that all field variables will assume equal values on opposite sides of the cell boundary. Therefore it is only necessary to consider a single cell in order to determine the dependence of these field variables on the microcoordinates x_i^*. As a consequence edge layer effects are not included in the model.

The construction of the present mixture model is accomplished by resorting to Reissner's mixed variational principle[28] for displacements and stresses. This variational principle, applied to the synthesized field using the multiscale representation, takes the form

$$\int_V\left[\sum_{\alpha=1}^{2}\int_{V^{*(\alpha)}}\left\{\delta e_{ij}^{(\alpha)}\hat{\sigma}_{ij}^{(\alpha)} + \delta\hat{\sigma}_{ij}^{(\alpha)}\left[\frac{1}{2}\left(u_{i,j}^{(\alpha)} + u_{j,i}^{(\alpha)} + \frac{1}{\varepsilon}(u_{i,j^*}^{(\alpha)} + u_{j,i^*}^{(\alpha)})\right) - e_{ij}^{(\alpha)}(\cdots)\right]\right\}\mathrm{d}x_1^*\,\mathrm{d}x_2^*\,\mathrm{d}x_3^*\right.$$

$$+ \frac{1}{\varepsilon}\int_{A_1}\left[\overset{v}{T_i'}(\delta u_i^{(2)} - \delta u_i^{(1)}) + \delta\overset{v}{T_i'}(u_i^{(2)} - u_i^{(1)})\right]\mathrm{d}A\bigg]\mathrm{d}x_1\,\mathrm{d}x_2\,\mathrm{d}x_3$$

$$= \int_V\left[\sum_{\alpha=1}^{2}\int_{V^{*(\alpha)}}\delta u_i^{(\alpha)}(-\rho^{(\alpha)}u_{i,tt}^{(\alpha)})\,\mathrm{d}x_1^*\,\mathrm{d}x_2^*\,\mathrm{d}x_3^*\right]\mathrm{d}x_1\,\mathrm{d}x_2\,\mathrm{d}x_3$$

$$+ \int_{\partial V_T}\left[\sum_{\alpha=1}^{2}\int_{V^{*(\alpha)}}\overset{v}{T_i^{(\alpha)}}\delta u_i^{(\alpha)}\,\mathrm{d}x_1^*\,\mathrm{d}x_2^*\,\mathrm{d}x_3^*\right]\mathrm{d}A$$
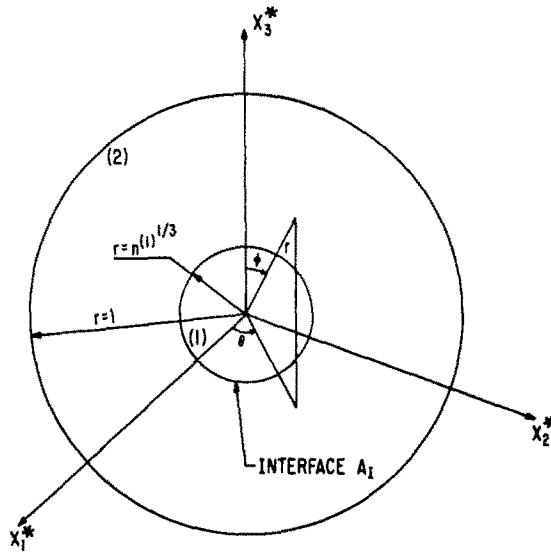
(12)

Fig. 2. Typical cell and concentric-spheres model.

where $V^{*(\alpha)}$ denotes the x_i^*-domain occupied by constituent α (see Fig. 2), $\hat{\sigma}_{ij}^{(\alpha)}$ is used for the approximate stress field, $\overset{v}{T}_i^{(\alpha)}$ represents the traction vector on the surface ∂V_T where tractions are specified and $\overset{v}{T}_i^{\prime}$ is the interface traction vector defined by

$$\overset{v}{T}_i^{\prime} \equiv \hat{\sigma}_{ji}^{(\alpha)} v_j^{(1)} \quad \text{on} \quad A_1. \tag{13}$$

Also

$$\delta e_{ij}^{(\alpha)} \equiv \frac{1}{2}\left[\delta u_{i,j}^{(\alpha)} + \delta u_{j,i}^{(\alpha)} + \frac{1}{\varepsilon}(\delta u_{i,j^*}^{(\alpha)} + \delta u_{j,i^*}^{(\alpha)})\right] \tag{14}$$

and

$$e_{ij}^{(\alpha)}(\cdots) = -\left[\frac{\lambda}{2\mu(3\lambda+2\mu)}\right]^{(\alpha)} \hat{\sigma}_{kk}^{(\alpha)}\delta_{ij} + \frac{1}{2\mu^{(\alpha)}}\hat{\sigma}_{ij}^{(\alpha)}. \tag{15}$$

3. ASYMPTOTIC ANALYSIS

The asymptotic technique starts by assuming the following expansions for the field variables:

$$\{u_i, \sigma_{ij}\}^{(\alpha)}(x_k, x_l^*, t; \varepsilon) = \sum_{n=0}^{\infty} \varepsilon^n \{u_{i(n)}, \sigma_{ij(n)}\}^{(\alpha)}(x_k, x_l^*, t); \quad \varepsilon \ll 1. \tag{16}$$

Substituting eqn (16) into the governing equations, eqns (8)–(11), and grouping terms in equal powers of ε, a sequence of problems is obtained. The first of these yields

$$u_{i(0),j^*}^{(\alpha)} = 0, \qquad \sigma_{ji(0),j^*}^{(\alpha)} = 0. \tag{17a, b}$$

Equation (17a) implies that $u_{i(0)}^{(\alpha)}$ are independent of the microcoordinates x_j^*. Together with the zeroth-order expansion of eqn (11a), one has then

$$u_{i(0)}^{(\alpha)} = U_{i(0)}(x_k, t). \tag{18}$$

The remaining sets of equations obtained from eqns (8)–(11), are, for $n \geqslant 0$

$$\sigma_{ji(n+1),j}^{(\alpha)} = \rho^{(\alpha)} u_{i(n),tt}^{(\alpha)} - \sigma_{ji(n),j}^{(\alpha)}, \qquad \sigma_{ji(n)}^{(\alpha)} = \sigma_{ij(n)}^{(\alpha)} \qquad (19a,b)$$

$$\sigma_{ij(n)}^{(\alpha)} = \lambda^{(\alpha)} e_{kk(n)}^{(\alpha)} \delta_{ij} + 2\mu^{(\alpha)} e_{ij(n)}^{(\alpha)} \qquad (20)$$

$$e_{ij(n)}^{(\alpha)} = \tfrac{1}{2}(u_{i(n),j}^{(\alpha)} + u_{j(n),i}^{(\alpha)} + u_{i(n+1),j}^{(\alpha)} + u_{j(n+1),i}^{(\alpha)}). \qquad (21)$$

Equations (19)–(21) are supplemented with interface continuity and x^*-periodicity conditions. These are, for $n \geqslant 0$

$$u_{i(n)}^{(1)} = u_{i(n)}^{(2)}, \qquad \sigma_{ji(n)}^{(1)} v_j^{(1)} = \sigma_{ji(n)}^{(2)} v_j^{(1)} \quad \text{on} \quad A_I \qquad (22a,b)$$

$$u_{i(n)}^{(2)} \quad \text{and} \quad \sigma_{ji(n)}^{(2)} v_j^{(2)} \quad \text{are } x^*\text{-periodic on the cell boundary.} \qquad (23a,b)$$

Equations (19)–(23) generate a series of microboundary value problems (MBVPs) for $\sigma_{ij(n)}^{(\alpha)}$ and $u_{i(n)}^{(\alpha)}$, which are to be solved sequentially. The first of the MBVPs, corresponding to $\sigma_{ij(0)}^{(\alpha)}$ and $u_{i(1)}^{(\alpha)}$, is called the $O(1)$ MBVPs and is defined by eqns (17b), (19b), (20), (21), (22b) and (23b) with $n = 0$ and eqns (22a) and (23a) with $n = 1$.

Higher order terms in the asymptotic expansions for the displacement and stress fields' microstructures, can be computed with suitable integrability and normalization conditions. However, due to the complexity of these MBVPs, a variational approach, based on Reissner's mixed principle[28] is preferred here in order to construct the mixture model. This construction can be carried out by supplying eqn (12) with appropriate trial displacement and stress fields which must satisfy the interface continuity condition (22) and the x^*-periodicity condition (23) on the cell boundary. As a result only approximate solutions of the MBVPs are necessary.

These trial functions are obtained by modeling the cell as two concentric spheres. This approximation of the cell geometry limits the applicability of the resulting mixture model to periodic particulate composites with cubic or hexagonal close-packed cells. However, the theory can easily be generalized at the cost of analytical simplicity for any arbitrary cell by introducing appropriate trial functions for the cell. The required trial functions may be computed by a finite element procedure proposed by Maewal[32]. The present concentric-spheres model is shown in Fig. 2 where (r, θ, ϕ) are spherical coordinates, such that

$$x_1^* = r \sin \phi \cos \theta$$
$$x_2^* = r \sin \phi \sin \theta \qquad (24)$$
$$x_3^* = r \cos \phi.$$

The volume of the cell is denoted by V^*, its boundary is defined by $r = 1$ and its interface surface by $r = (n^{(1)})^{1/3}$. The quantities $n^{(\alpha)}$ denote the volume fraction of material α and satisfy the relation

$$n^{(1)} + n^{(2)} = 1. \qquad (25)$$

In terms of the spherical coordinates (r, θ, ϕ), the x^*-periodicity condition for the concentric-spheres approximation can be expressed as

$$F(r, \theta, \phi) = F(r, \pi + \theta, \pi + \phi). \qquad (26)$$

4. TRIAL DISPLACEMENT AND STRESS FIELDS

The $O(1)$ stress and $O(\varepsilon)$ displacement fields can be determined by solving the $O(1)$ MBVPs which are defined by eqns (17b), (19b) and (20)–(23). As shown in Ref. [29], these MBVPs are excited by $U_{i(0),j}$. Therefore, the mixture formulation becomes more tractable by introducing microdisplacement variables which represent $U_{i(0),j} + U_{j(0),i}$, such that

$$\overset{j}{S_i}(x_k, t) \equiv \frac{1}{\varepsilon V^*} \int_{A_1} u_i^{(\alpha)} v_j^{(1)} \, \mathrm{d}A^* = \frac{1}{V^*} \int_{A_1} u_{i(1)}^{(\alpha)} v_j^{(1)} \, \mathrm{d}A^* \tag{27}$$

where V^* is the volume of the cell. Since $u_{i(1)}^{(\alpha)}$ is excited by $U_{i(0),j} + U_{j(0),i}$ there holds

$$\overset{j}{S_i} = \overset{i}{S_j}. \tag{28}$$

As an $O(\varepsilon)$ trial displacement field, the following form may be used:

$$u_{i(1)}^{(\alpha)} = \overset{j}{S_i}(x_k, t) g_j^{(\alpha)}(x_l^*) \tag{29a}$$

where

$$g_i^{(\alpha)}(x_j^*) = \frac{1}{n^{(\alpha)}} \left[(-1)^{\alpha+1} x_i^* + \delta_{\alpha 2} \frac{x_i^*}{r^3} \right]. \tag{29b}$$

Considering the $O(\varepsilon^2)$ difference of the average of $u_i^{(\alpha)}$ over $V^{*(\alpha)}$, eqns (18) and (29) yield the following trial displacement field

$$u_i^{(\alpha)}(x_k, x_l^*, t, \varepsilon) = U_i^{(\alpha)}(x_k, t) + \varepsilon u_{i(1)}^{(\alpha)}(x_k, x_l^*, t) \tag{30}$$

where $u_{i(1)}^{(\alpha)}$ is given by eqn (29). Equations (29) and (30) show that the mixture displacement variables are $U_i^{(1)}$, $U_i^{(2)}$, $\overset{j}{S_i}$ subject to the constraint (28). Inserting eqn (30) into eqns (20) and (21) with $n = 0$ and considering the $O(\varepsilon^2)$ differences of the average stresses, the $O(1)$ trial stress field may be written as

$$\hat{\sigma}_{ij(0)}^{(\alpha)} = \tau_{ij}^{(\alpha)}(x_k, t) + \tau_{ijkl}^{(\alpha)}(x_p, t) g_{k,l}^{(\alpha)}. \tag{31}$$

As with displacement variables, $O(\varepsilon)$ stress variables are conveniently introduced according to

$$P_i(x_k, t) \equiv \frac{1}{\varepsilon V^*} \int_{A_1} \sigma_{ji}^{(\alpha)} v_j^{(1)} \, \mathrm{d}A^* = \frac{1}{V^*} \int_{A_1} \sigma_{ji(1)}^{(\alpha)} v_j^{(1)} \, \mathrm{d}A^*. \tag{32}$$

Integrating eqn (8a) over $V^{*(\alpha)}$ and making use of the x^*-periodicity condition, the following mixture equation is obtained:

$$n^{(\alpha)} \sigma_{ji,j}^{(\alpha a)} + (-1)^{\alpha+1} P_i = n^{(\alpha)} \rho^{(\alpha)} u_{i,tt}^{(\alpha a)} \tag{33}$$

where the average operation is defined by

$$F^{(\alpha a)}(x_k, t) \equiv \frac{1}{n^{(\alpha)} V^*} \int_{V^{*(\alpha)}} F^{(\alpha)}(x_k, x_j^*, t) \, \mathrm{d}x_1^* \, \mathrm{d}x_2^* \, \mathrm{d}x_3^*. \tag{34}$$

From eqn (33) it is seen that P_i plays the role of an interaction body force between the two constituents through the interface.

As an $O(\varepsilon)$ trial stress field, the following form may be used:

$$\hat{\sigma}_{ij(1)}^{(\alpha)}(x_k, x_l^*, t) = P_n(x_k, t) g_n^{(\alpha)}(x_l^*) \delta_{ij}. \tag{35}$$

As a result, the trial stress field may now be written in the form

$$\hat{\sigma}_{ij}^{(\alpha)}(x_k, x_l^*, t, \varepsilon) = \hat{\sigma}_{ij(0)}^{(\alpha)}(x_k, x_l^*, t) + \varepsilon \hat{\sigma}_{ij(1)}^{(\alpha)}(x_k, x_l^*, t) \tag{36}$$

where $\hat{\sigma}_{ij(0)}^{(\alpha)}$ and $\hat{\sigma}_{ij(1)}^{(\alpha)}$ are defined by eqns (31) and (35), respectively.

5. MIXTURE EQUATIONS

Substituting the trial displacement and stress fields defined by eqns (30) and (36), respectively, into Reissner's mixed variational principle, eqn (12), and using eqns (14) and (15), the following governing equations are obtained:

(a) Equations of motion

$$n^{(\alpha)} \tau_{ji,j}^{(\alpha)} + (-1)^{\alpha + 1} \tau_{jikk,j}^{(\alpha)} + (-1)^{\alpha + 1} P_i = n^{(\alpha)} \rho^{(\alpha)} U_{i,tt}^{(\alpha)} \tag{37a}$$

$$\frac{1}{\varepsilon^2} \left[\tau_{ij}^{(2)} - \tau_{ij}^{(1)} - \frac{1}{n^{(1)}} \tau_{ijkk}^{(1)} - \frac{1}{n^{(2)}} \tau_{ijkk}^{(2)} - \kappa_{mlkj} \tau_{ikml}^{(2)} \right] + A_1 P_{j,i} = A_2 \overset{j}{S}_{i,tt} \tag{37b}$$

where

$$(A_1, A_2) \equiv \sum_{\alpha=1}^{2} A^{(\alpha)}(1, \rho^{(\alpha)}) \tag{38a}$$

and

$$A^{(\alpha)} = \frac{1}{n^{(\alpha)2}} \left[\frac{1}{5} (-1)^{\alpha + 1} n^{(1)5/3} + \delta_{\alpha 2} \left(\frac{n^{(1)} + 1}{n^{(1)1/3}} - \frac{9}{5} \right) \right]. \tag{38b}$$

Also κ_{mlkj} are constants that depend on $n^{(1)}$ and $n^{(2)}$ only. The non-zero values of these constants are given in the Appendix. It should be noted that in eqn (37), the superscript "a" used to denote "average" has been dropped from $\tau_{ij}^{(\alpha)}$ and $\tau_{ijkl}^{(\alpha)}$ since these are independent of the microcoordinates x_l^*.

(b) Constitutive equations

$$\tau_{ij}^{(\alpha)} = \lambda^{(\alpha)} U_{k,k}^{(\alpha)} \delta_{ij} + \mu^{(\alpha)} (U_{i,j}^{(\alpha)} + U_{j,i}^{(\alpha)}) \tag{39a}$$

$$\tau_{ijlk}^{(\alpha)} = \lambda^{(\alpha)} \overset{l}{S}_k \delta_{ij} + \mu^{(\alpha)} (\delta_{kj} \overset{l}{S}_i + \delta_{ki} \overset{l}{S}_j) \tag{39b}$$

$$P_i = A_3 \left(\frac{U_i^{(2)} - U_i^{(1)}}{\varepsilon^2} + A_1 \overset{i}{S}_{k,k} \right) \tag{39c}$$

where

$$A_3 \equiv 1 \bigg/ \left[3 \sum_{\alpha=1}^{2} \left(\frac{A^{(\alpha)}}{3\lambda^{(\alpha)} + 2\mu^{(\alpha)}} \right) \right]. \tag{40}$$

(c) Boundary conditions along ∂V

$$\delta U_i^{(\alpha)} = 0 \quad \text{or} \quad n^{(\alpha)} \tau_{ij}^{(\alpha)} v_j + (-1)^{\alpha + 1} \tau_{ijkk}^{(\alpha)} v_j = \overset{v}{T}_i^{(\alpha p)} \tag{41a}$$

$$\delta \overset{j}{S}_i = 0 \quad \text{or} \quad A_1 P_j v_i = \overset{vj}{T}_i \tag{41b}$$

where

$$\overset{v}{T}_i^{(\alpha p)} \equiv \frac{1}{V^*} \int_{V^{*(\alpha)}} \overset{v}{T}_i^{(\alpha)} \, dx_1^* \, dx_2^* \, dx_3^* \tag{42a}$$

$$\overset{vj}{T}_i \equiv \frac{1}{V^*} \sum_{\alpha=1}^{2} \int_{V^{*(\alpha)}} \overset{v}{T}_i^{(\alpha)} g_j^{(\alpha)} \, dx_1^* \, dx_2^* \, dx_3^*. \tag{42b}$$

(d) Initial conditions

$$\text{specify} \quad U_i^{(\alpha)}, \quad U_{i,t}^{(\alpha)}, \quad \overset{j}{S}_i, \quad \overset{j}{S}_{i,t} \quad \text{at} \quad t = 0. \tag{43}$$

Equations (37), (39), (41) and (43) constitute a well-posed boundary value problem with respect to time t and macrocoordinates x_k.

6. EFFECTIVE ELASTIC MODULI

The effective elastic moduli, which relate stress averages to strain averages, are defined by the $O(1)$ homogenization theory. They can thus be obtained by letting $\varepsilon \to 0$ in eqns (37) and setting

$$U_i^{(1)} = U_i^{(2)} = U_i. \tag{44}$$

Equation (37a) yields

$$\sigma_{ij}^{(m)} = \rho^{(m)} U_{i,tt} \tag{45}$$

where

$$\sigma_{ij}^{(m)} \equiv \sum_{\alpha=1}^{2} [n^{(\alpha)} \tau_{ij}^{(\alpha)} + (-1)^{\alpha+1} \tau_{ijkk}^{(\alpha)}] \tag{46a}$$

$$\rho^{(m)} \equiv \sum_{\alpha=1}^{2} n^{(\alpha)} \rho^{(\alpha)} \tag{46b}$$

while eqn (37b) yields

$$\tau_{ij}^{(2)} - \tau_{ij}^{(1)} - \frac{1}{n^{(1)}} \tau_{ijkk}^{(1)} - \frac{1}{n^{(2)}} \tau_{ijkk}^{(2)} - \kappa_{mlkj} \tau_{ikml}^{(2)} = 0. \tag{47}$$

This last equation can be solved for $\overset{j}{S}_i$ by inserting therein eqns (39a) and (39b). Substituting in turn these expressions for $\overset{j}{S}_i$ into eqn (46a), one obtains

$$\boldsymbol{\sigma}^{(m)} = [C^{(m)}] \mathbf{e}^{(m)} \tag{48}$$

where

$$\boldsymbol{\sigma}^{(m)} = [\sigma_{11}, \sigma_{22}, \sigma_{33}, \sigma_{23}, \sigma_{31}, \sigma_{12}]^T \tag{49a}$$

$$\mathbf{e}^{(m)} = [U_{1,1}, U_{2,2}, U_{3,3}, U_{2,3} + U_{3,2}, U_{3,1} + U_{1,3}, U_{1,2} + U_{2,1}]^T \tag{49b}$$

and $[C^{(m)}]$ is the effective elastic modulus matrix. Although the medium is heterogeneous, it is isotropic. Consequently, only two independent constants should suffice, as is indeed the case. $[C^{(m)}]$ is conveniently written in the standard form
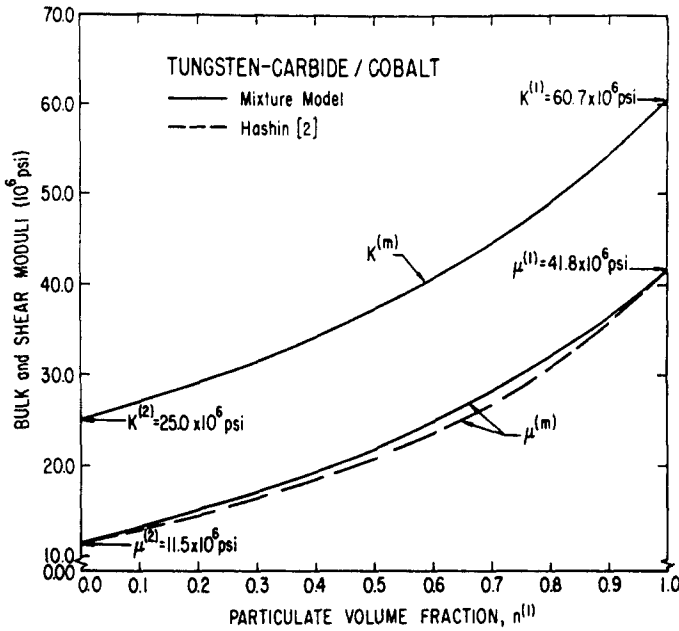
Fig. 3. Bulk and shear moduli as a function of particulate volume fraction.

$$[C^{(m)}] = \begin{bmatrix} \lambda+2\mu & \lambda & \lambda & 0 & 0 & 0 \\ \lambda & \lambda+2\mu & \lambda & 0 & 0 & 0 \\ \lambda & \lambda & \lambda+2\mu & 0 & 0 & 0 \\ 0 & 0 & 0 & \mu & 0 & 0 \\ 0 & 0 & 0 & 0 & \mu & 0 \\ 0 & 0 & 0 & 0 & 0 & \mu \end{bmatrix}^{(m)}. \tag{50}$$

The composite Lame's constants $\lambda^{(m)}$ and $\mu^{(m)}$ are given in the Appendix.

In order to assess the accuracy of the present $O(1)$ mixture theory, the results for the elastic constants of a tungsten carbide/cobalt particulate composite are presented and compared with those obtained by Hashin[2]. Young's modulus E and Poisson's ratio v are

$$\text{for tungsten carbide} \quad \bar{E}^{(1)} = 102 \times 10^6 \text{ psi}, \quad v^{(1)} = 0.22 \tag{51a}$$

$$\text{and for cobalt} \quad \bar{E}^{(2)} = 30 \times 10^6 \text{ psi}, \quad v^{(2)} = 0.30. \tag{51b}$$

The variations in terms of the particle volume fraction $n^{(1)}$ of the composite bulk modulus $K^{(m)}$ and shear modulus $\mu^{(m)}$ are shown in Fig. 3, where very good agreement is observed with Hashin's results[2]. For the bulk modulus $K^{(m)}$, the two curves are identical. The expression for $K^{(m)}$ derived by Hashin[2] represents an exact result when the medium is completely filled out with concentric spheres. It should be emphasized here that the effective medium is isotropic because the shape of the composite unit cell has been modeled as being spherical. Had one used a cubic cell instead, then as shown by Iwakuma and Nemat-Nasser[15] and Nunan and Keller[33], the elasticity tensor would have had three independent coefficients as compared to two coefficients for the spherical cell model.

7. HARMONIC WAVE PROPAGATION

In order to test the accuracy of the present $O(\varepsilon)$ mixture model, phase velocity spectra have been compared with experimental data for harmonic wave propagation. Due to the composite isotropy, it is sufficient to consider harmonic waves propagating along, say, the x_1-direction. Therefore, let

$$\left\{ U_i^{(\alpha)}(x_k, t),\ \overset{j}{S_i}(x_k, t) \right\} = \left\{ \hat{U}_i^{(\alpha)},\ (ik)\overset{j}{S_i^*} \right\} e^{(ikx_1 - i\omega t)} \tag{52}$$

where $\hat{U}_i^{(\alpha)}$ and $\overset{j}{S_i^*}$ represent constant amplitudes. Also, k and ω denote the wave number and the angular frequency, respectively.

Substituting eqn (52) into eqn (37) and using the constitutive equations, eqns (39), yields an eigenvalue problem for $(\varepsilon\omega)$ of the form

$$[K]U = (\varepsilon\omega)^2[M]U \tag{53}$$

where

$$U = \left[\hat{U}_1^{(1)}, \hat{U}_1^{(2)}, \overset{1}{S_1^*}, \overset{2}{S_2^*}, \overset{3}{S_3^*}, \hat{U}_2^{(1)}, \hat{U}_2^{(2)}, \overset{2}{S_1^*}, \hat{U}_3^{(1)}, \hat{U}_3^{(2)}, \overset{3}{S_1^*}, \overset{3}{S_2^*} \right]^T \tag{54}$$

$[K]$ and $[M]$ are (12×12) real symmetric matrices, whose elements are functions of the volume fractions, constituents' elastic properties and wave number. Furthermore, $[M]$ is a diagonal matrix. Equation (53) reveals that for a given (εk), there corresponds 12 eigenvalues $(\varepsilon\omega)$. The phase velocity C_p is then determined from

$$C_p = \frac{(\varepsilon\omega)}{(\varepsilon k)}. \tag{55}$$

In the present analysis the typical cell dimension $\bar{\Delta}$ was chosen to be the cell radius by using the concentric-spheres model. The reference elastic modulus and density used for the nondimensionalization are

$$\bar{E}_{(m)} = \sum_{\alpha=1}^{2} n^{(\alpha)} \bar{E}^{(\alpha)}, \qquad \bar{\rho}_{(m)} = \sum_{\alpha=1}^{2} n^{(\alpha)} \bar{\rho}^{(\alpha)}. \tag{56}$$

The dimensional frequency f(Hz) is then given by

$$f = \frac{(\varepsilon\omega)}{2\pi\bar{\Delta}} \sqrt{\left(\frac{\bar{E}_{(m)}}{\bar{\rho}_{(m)}} \right)}. \tag{57}$$

Numerical results were obtained for two composites: glass/epoxy and steel/PMMA, for which experimental data have been recorded by Kinra and Ker[18] for longitudinal waves. The constituents' physical properties are given in Table 1, in which the values for Poisson's ratio are estimates. In the simulation $\bar{\Delta}$ was computed from the particle's radius which was 1 mm for glass and 0.55 mm for steel.

Table 1. Physical properties for glass/epoxy and steel/PMMA composites

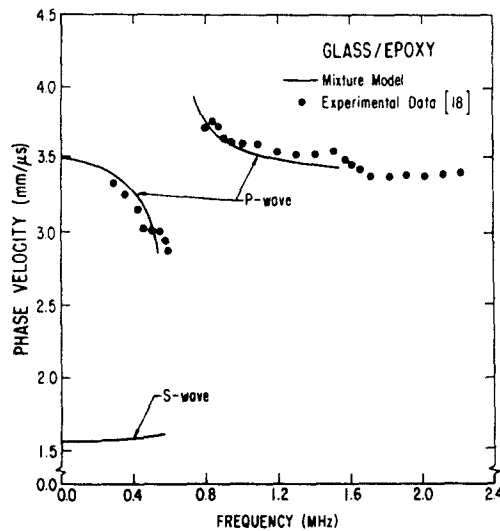|	Volume fraction $n^{(\alpha)}$	Young's modulus $E^{(\alpha)}$ (GPa)	Poisson's ratio $\nu^{(\alpha)}$	Mass density $\bar{\rho}^{(\alpha)}$ (g cm^{-3})
(1) Glass	0.256	62.784	0.20	2.492
(2) Epoxy	0.744	4.541	0.43	1.18
(1) Steel	0.152	113.534	0.292	7.8
(2) PMMA	0.848	3.032	0.30	1.16

Fig. 4. Phase velocity as a function of frequency in glass/epoxy composite.
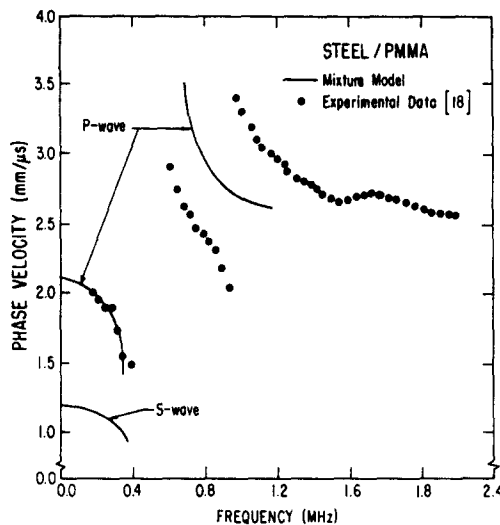

Fig. 5. Phase velocity as a function of frequency in steel/PMMA composite.

Phase velocity profiles for each composite are shown in Figs 4 and 5, where two distinct modes are displayed: a longitudinal (P-mode) wave and a shear (S-mode) wave.

For a given (εk) the number of eigenvalues $(\varepsilon \omega)$ depends on the number of displacement variables introduced in the trial functions for $u_i^{(\alpha)}$. In the present case, computations yield five branches for the P-mode and three branches for each S-mode. The first two branches in the spectrum for the P-mode, which are believed to be sufficiently accurate within the present calculation, are plotted as functions of frequency. Figures 4 and 5 clearly bring out the dispersive characteristic of the composite. The experimental data correspond to the longitudinal mode, and it can be seen that the correlation with the present results is quite satisfactory. In their paper, Kinra and Ker[18] have predicted, at higher frequencies where the wavelength approaches the particle's radius, additional second ($f = 1.4$ MHz) and third ($f = 2.0$ MHz) stop bands for glass/epoxy, and additional third ($f = 1.5$ MHz) and fourth ($f = 1.9$ MHz) stop bands for steel/PMMA. Their experiments however did not reveal these higher stop bands. They have conjectured "that this is probably due to the excitation of resonances of the spherical inclusions which, at higher frequencies, tend to dominate the resonances of the unit cell". Figure 4 (glass/epoxy) shows an additional stop band at $f = 1.53$ MHz, which is in fairly close agreement with the value predicted by Kinra and Ker[18]. (The remaining three branches given by the mixture model corresponding to the P-mode are *not* shown in the figures.)

Finally, for completeness, the first branch of the shear wave velocity spectrum is also shown in Figs 4 and 5, for each composite. Due to the composite isotropy, the vertically (SV) and horizontally (SH) polarized wave speeds are identical.

8. CONCLUSION

A micromechanical mixture model for periodic particulate composites was presented based on a two-scale asymptotic expansion. Governing equations and appropriate boundary conditions were deduced from Reissner's mixed variational principle[28]. Expressions for the effective elastic moduli were derived and compared with Hashin's results[2]. Also, harmonic wave dispersion spectra were obtained, and a good correlation with the experimental data of Kinra and Ker[18] for glass/epoxy and steel/PMMA composites was observed.

REFERENCES

1. R. M. Christensen, *Mechanics of Composite Materials*. Wiley-Interscience, New York (1979).
2. Z. Hashin, The elastic moduli of heterogeneous materials. *ASME J. Appl. Mech.* 29, 143–150 (1962).
3. Z. Hashin and S. Shtrikman, A variational approach to the theory of the elastic behaviour of multiphase materials. *J. Mech. Phys. Solids* 11, 127–140 (1963).
4. L. J. Walpole, On bounds for the overall elastic moduli of inhomogeneous systems—I. *J. Mech. Phys. Solids* 14, 151–162 (1966).
5. M. N. Miller, Bounds for effective bulk modulus of heterogeneous materials. *J. Math. Phys.* 10, 2005–2013 (1969).
6. G. K. Batchelor and J. T. Green, The determination of the bulk stress in a suspension of spherical particles to order c^2. *J. Fluid Mech.* 56, 401–427 (1972).
7. D. J. Jeffrey, Group expansions for the bulk properties of a statistically homogeneous, random suspension. *Proc. R. Soc. Lond.* A338, 503–516 (1974).
8. H. S. Chen and A. Acrivos, The solution of the equations of linear elasticity for an infinite region containing two spherical inclusions. *Int. J. Solids Structures* 14, 331–348 (1978).
9. H. S. Chen and A. Acrivos, The effective elastic moduli of composite materials containing spherical inclusions at non-dilute concentrations. *Int. J. Solids Structures* 14, 349–364 (1978).
10. R. Hill, A self-consistent mechanics of composite materials. *J. Mech. Phys. Solids* 13, 213–222 (1965).
11. B. Budiansky, On the elastic moduli of some heterogeneous materials. *J. Mech. Phys. Solids* 13, 223–227 (1965).
12. T. T. Wu, The effect of inclusion shape on the elastic moduli of a two-phase material. *Int. J. Solids Structures* 2, 1–8 (1966).
13. R. M. Christensen and K. H. Lo, Solutions for effective shear properties in three phase sphere and cylinder models. *J. Mech. Phys. Solids* 27, 315–330 (1979).
14. S. Nemat-Nasser and M. Taya, On effective moduli of an elastic body containing periodically distributed voids. *Q. Appl. Math.* 39, 43–59 (1981).
15. T. Iwakuma and S. Nemat-Nasser, Composites with periodic microstructure. *Comput. Struct.* 16(1–4), 13–19 (1983).
16. V. K. Kinra, M. S. Petraitis and S. K. Datta, Ultrasonic wave propagation in a random particulate composite. *Int. J. Solids Structures* 16, 301–312 (1980).
17. V. K. Kinra and A. Anand, Wave propagation in a random particulate composite at long and short wavelengths. *Int. J. Solids Structures* 18, 367–380 (1982).
18. V. K. Kinra and E. L. Ker, An experimental investigation of pass bands and stop bands in two periodic particulate composites. *Int. J. Solids Structures* 19, 393–410 (1983).
19. S. Minagawa and S. Nemat-Nasser, Harmonic waves in three-dimensional elastic composites. *Int. J. Solids Structures* 12, 769–777 (1976).
20. A. K. Mal and S. K. Bose, Dynamic elastic moduli of a suspension of imperfectly bonded spheres. *Proc. Camb. Phil. Soc.* 76, 587–600 (1974).
21. S. K. Datta, Scattering of elastic waves by a distribution of inclusions. *Archs Mech.* 28, 317–324 (1976).
22. S. K. Datta, A self-consistent approach to multiple scattering by elastic ellipsoidal inclusions. *ASME J. Appl. Mech.* 44, 657–662 (1977).
23. A. I. Beltzer, C. W. Bert and A. G. Striz, On wave propagation in random particulate composites. *Int. J. Solids Structures* 19, 785–791 (1983).
24. M. Ben-Amoz, A dynamic theory for composite materials. *J. Appl. Math. Phys. (ZAMP)* 27, 83–99 (1976).
25. G. C. Gaunard and H. Überall, Resonance effects and the ultrasonic effective properties of particulate composites. *J. Acoust. Soc. Am.* 74, 305–313 (1983).
26. H. Murakami, A mixture theory for wave propagation in angle-ply laminates, Part I: theory. *ASME J. Appl. Mech.* 52, 331–337 (1985).
27. H. Murakami and G. A. Hegemier, A mixture model for unidirectionally fiber-reinforced composites, *ASME J. Appl. Mech.* 53, 765–773 (1986).

28. E. Reissner, On a variational theorem in elasticity. *J. Math. Phys.* **29**, 90–95 (1950).
29. A. Bensoussan, J. L. Lions and G. Papanicolaou, *Asymptotic Analysis for Periodic Structures*. North-Holland, Amsterdam (1978).
30. E. Sanchez-Palencia, *Non-homogeneous Media and Vibration Theory*, Lecture Notes in Physics 127. Springer, Berlin (1980).
31. R. Burridge and J. B. Keller, Poroelasticity equations derived from microstructure. *J. Acoust. Soc. Am.* **70**, 1140–1146 (1981).
32. A. Maewal, Construction of models of dispersive elastodynamic behavior of periodic composites: a computational approach. *Comput. Meth. Appl. Mech. Engng* **57**, 191–205 (1986).
33. K. C. Nunan and J. B. Keller, Effective elasticity tensor of a periodic composite. *J. Mech. Phys. Solids* **32**, 259–280 (1984).

APPENDIX

(a) Non-zero values of constants κ_{mikj} appearing in eqn (37b)

$$\kappa_{iiii} = \frac{1}{5n^{(1)}n^{(2)}} ; \quad \text{no sum on } i \tag{A1}$$

$$\kappa_{iijj} = \kappa_{jjii} = \frac{1}{15n^{(1)}n^{(2)}} ; \quad i \neq j, \quad \text{no sum on } i \text{ and } j \tag{A2}$$

$$\kappa_{ijij} = \kappa_{ijji} = \kappa_{jiij} = \kappa_{jiji} = \frac{3}{5n^{(1)}n^{(2)}} ; \quad i \neq j, \quad \text{no sum on } i \text{ and } j. \tag{A3}$$

(b) Expression for composite Lame's constants $\lambda^{(m)}$ and $\mu^{(m)}$ appearing in eqn (50)

$$\begin{aligned}
\lambda^{(m)} &= \hat{\lambda} + (3a_1 + 2a_2)\rho_1 + 2a_1\rho_2 \\
\mu^{(m)} &= \hat{\mu} + 2a_2\rho_2
\end{aligned} \tag{A4}$$

where

$$\begin{aligned}
(\hat{\lambda}, \hat{\mu}) &\equiv \sum_{\alpha=1}^{2} n^{(\alpha)}(\lambda^{(\alpha)}, \mu^{(\alpha)}) \\
a_1 &\equiv \lambda^{(1)} - \lambda^{(2)}, \qquad a_2 \equiv \mu^{(1)} - \mu^{(2)} \\
\rho_1 &\equiv \frac{-a_1\beta + (a_1 + 2a_2)\gamma}{\beta^2 - 2\gamma^2 + \beta\gamma}, \qquad \rho_2 \equiv \frac{-a_2}{\beta - \gamma}
\end{aligned} \tag{A5}$$

and

$$\begin{aligned}
\beta &\equiv \sum_{\alpha=1}^{2} \left(\frac{\lambda^{(\alpha)} + 2\mu^{(\alpha)}}{n^{(\alpha)}} \right) + \frac{2(2\lambda^{(2)} + 7\mu^{(2)})}{5n^{(1)}n^{(2)}} \\
\gamma &\equiv \sum_{\alpha=1}^{2} \left(\frac{\lambda^{(\alpha)}}{n^{(\alpha)}} \right) + \frac{(3\mu^{(2)} - 2\lambda^{(2)})}{5n^{(1)}n^{(2)}}.
\end{aligned} \tag{A6}$$